Available online at www.sciencedirect.com
SCIENCE DIRECT
International Journal of Mass Spectrometry 251 (2006) 23–31
International Journal of Mass Spectrometry
www.elsevier.com/locate/ijms

Hydration of gas-phase protonated alkylamines, amino acids and dipeptides produced by electrospray

Henryk Wincel *

Department of Chemical Dynamics, Institute of Physical Chemistry, Polish Academy of Sciences, Kasprzaka 44/52, 01-224 Warsaw, Poland

Received 10 November 2005; received in revised form 14 December 2005; accepted 14 December 2005
Available online 25 January 2006

Dedicated to Prof. D.K. Bohme on the occasion of his 65th birthday.

Abstract

An electrospray ionization ion source is described that produces ions continuously at 1 atm and introduces them into a temperature-variable reaction chamber in the pulsed mode where the ion–molecule equilibria can be determined in the gas phase at 10 mbar. Technical aspects and operating parameters of the technique are presented. The equilibrium constants for the hydration reactions $B^+(H_2O)_{n-1} + H_2O = B^+(H_2O)_n$, where $B^+ = (CH_3)_2NH_2^+$, $C_2H_5NH_3^+$, n-$C_4H_9NH_3^+$, GluH$^+$, MetH$^+$, ValH$^+$, (Glu-Met)H$^+$ and (Met-Glu)H$^+$, were determined with a magnetic mass spectrometer, and the thermochemical properties, $\Delta H^\circ_{n-1,n}$, $\Delta S^\circ_{n-1,n}$ and $\Delta G^\circ_{n-1,n}$, for these reactions were determined and discussed. The results obtained with the present technique for protonated alkylamines are compared with previously published values, demonstrating the usefulness of this technique for quantitative measurements of the gas phase ion thermochemistry based on ion–molecule equilibria. A correlation between the free energy changes for the attachment of the first water molecule to the protonated amino acids and the corresponding gas-phase basicities is obtained.

Keywords: Gas-phase equilibria; Bond enthalpies; Biomolecules hydration; Electrospray

1. Introduction

The study of the thermochemical properties of gas phase cluster ions provides detailed information on microscopic interactions of ions with solvent molecules without interference arising from the presence of the bulk solvent. Due to the limitations of "conventional" ionization techniques, most of these studies have long been restricted to small ions. The development of electrospray ionization (ESI) by Fenn et al. [1] provided the apparent ability to "softly" transfer ionized species of non-volatile and thermally labile molecules from the solution to the gas phase. ESI has greatly extended the range of compounds that can be studied by mass spectrometry and also provided new possibilities of studying the stepwise solvation of biomolecule ions in the gas phase.

Hydration of biomolecules is one of the most important problems in biology. Water is known to be a vital part of a functioning biological system. A minimum amount of water is necessary to awaken biological activity in enzymes and dried proteins. The fact that in the gas phase the most stable form of isolated amino acids is non-zwitterions, but in aqueous solutions they exist as zwitterions over a wide range of pH, suggests that hydration drives their transformation, and also provides stabilization of the zwitterionic structures.

Many biologically important compounds such as amino acids and peptides are present in ionic form in vivo. To gain a better understanding of the interaction of water with large biomolecules, knowledge of binding energies to smaller systems is required. Protonated amino acids and small peptides provide a simple model for biologically relevant hydration studies. Such studies provide a bridge between the gas-phase and solution properties of biomolecules and can lead to an improved understanding of the structure and functions of biomolecules in which water interactions play a role.

The distribution of extensively hydrated peptides generated by electrospray ionization has been studied [2–4]. Several laboratories developed mass spectrometric techniques with ESI to study the stepwise hydration of polyatomic ions such as amines

* Tel.: +48 22 343 3253; fax: +48 22 632 5276.
E-mail address: wincel@ichf.edu.pl.

1387-3806/$ – see front matter © 2006 Elsevier B.V. All rights reserved.
doi:10.1016/j.ijms.2005.12.036

and biomolecules under high-pressure equilibrium conditions [5–9]. Thermochemical data on the binding of water molecules to protonated alkylamines [6,9–13], amino acids [5,14,15], peptides [5,16–19] and proteins [7,20] have been reported.

This paper describes an ion source in which the ion beam generated by electrospray is pulsed into a temperature-variable reaction chamber. The source can be used to study the stepwise hydration of biomolecule ions and energetics for sequential steps of solvation from the gas-phase equilibria measurements. A number of experimental parameters have been examined and the thermochemical properties for the hydration of a few protonated alkylamines have been determined and compared with literature values in order to test the reliability of the method. New experimental determinations of the hydration energies for the protonated amino acids, $GluH^+$, $ValH^+$ and $MetH^+$, and dipeptides, $(Glu\text{-}Met)H^+$ and $(Met\text{-}Glu)H^+$, are also reported.

2. Experimental

Some years ago, we constructed a pulsed electron-beam high-pressure mass spectrometer operated with a 60° magnetic sector analyzer [21]. This instrument has been modified to work with an ESI source. A schematic diagram of the homemade ion source is shown in Fig. 1. The ions are generated at atmospheric pressure by a microelectrospray emitter made from a fused-silica capillary, ESC (15 μm i.d.; 150 μm o.d.), inserted into a stainless steel capillary from which the emitter extended 2 mm. To provide electrical contact, the emitter end (∼10 mm) is coated with a conductive polyimide/graphite mixture following the procedure described by Nilsson et al. [22]. After the coating, the polyimide mixture was cured for 10 min at 250 °C. The ESI emitter prepared in this manner is mounted on a home-built manipulator. Sample solutions are delivered to the electrospray needle by a syringe pump (Ascor apparatus, Model 11a) from a glass syringe (0.5 mL Hamilton) at a flow rate of 0.8 μL/min. All solutions were prepared at a concentration of $\sim 1 \times 10^{-4}$ M in CH_3OH. The electrospray tip is positioned about 5 mm from the orifice (4 mm diameter) in the curtain plate, CP, which is electrically isolated from the stainless steel pressure reduction capillary, PRC, kept at the potential of the reaction chamber, RC. A counter-current flow of nitrogen curtain gas with a flow rate of ∼25 L/h was supplied through the curtain gas inlet (CGI).

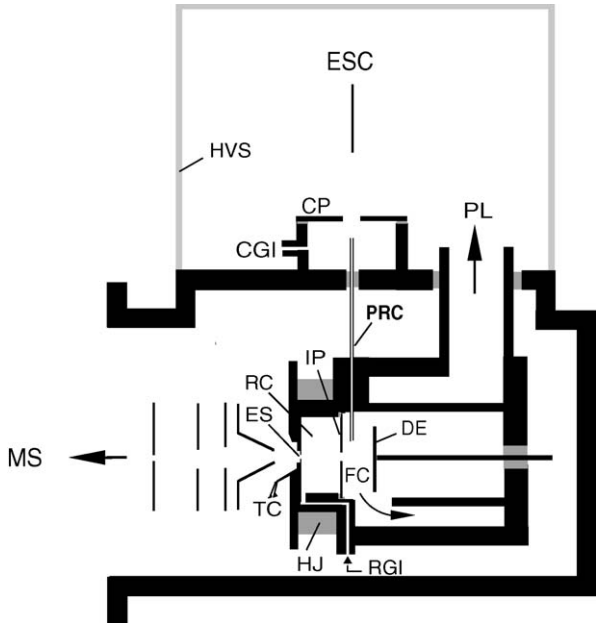

Fig. 1. Scheme of the combined electrospray emitter and high-pressure ion source with pulsed ion beam: (ESC) electrospray capillary; (HVS) high voltage shield; (CP) curtain plate; (CGI) curtain gas inlet; (PL) pumping lead; (PRC) pressure reducing capillary; (FC) forechamber; (DE) deflection electrode; (IP) interface plate; (RC) reaction chamber; (RGI) reactant gas inlet; (TC) thermocouple; (ES) exit slit; (HJ) electrically heated jacket.

The design of the reaction chamber is similar in concept to that developed by Kebarle and co-workers [5]. However, the present ESI source contains two important features which represent a distinct improvement over the others [5,9]: (1) the pressure reducing capillary, PRC (0.5 mm i.d.; 118 mm long), which introduces the ions generated by electrospray into the forechamber, FC, is resistively heated (80–200 °C) and serves as the desolvation capillary. The distances from the exit of PRC to the interface plate, IP, and the deflection electrode, DE, are 2 and 5 mm, respectively, and 5 mm from the axis of the orifice in IP. (2) The electrodes DE and IP are electrically insulated. With $V_{DE} = V_{IP}$, by applying short pulses to the electrode DE, narrow "slices" of the continuous ion beam entering the FC can be periodically injected into the reaction chamber, RC (7 mm length; 20 mm i.d.), through a 3 mm orifice in IP. This mode of operation allows measurements of the arrival time distribution (ATD) of ions moving across the RC toward the exit slit, ES (15 μm × 3 mm), under the influence of a small potential applied to the IP. As an example, Fig. 2 shows several arrival time distributions obtained for a non-reacting $GluH^+$ in N_2 bath gas at various values of the electric field strength, E. These distributions show that the peak is broadened by longitudinal diffusion as the mean drift time (equal to the reaction time) increases with decreasing E. The drift velocity v_d of an ion packet is propor-

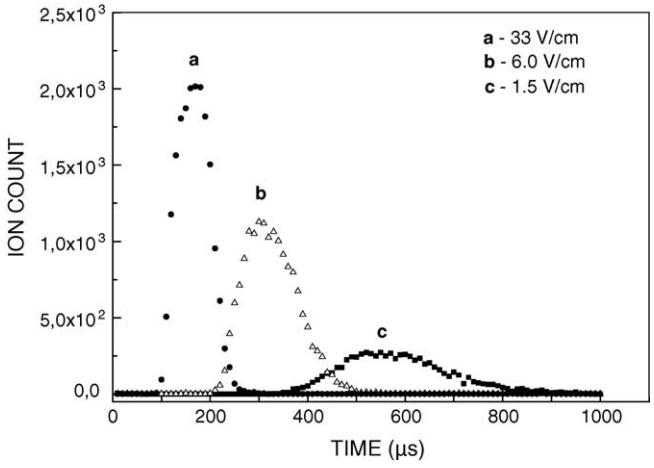

Fig. 2. Arrival time distributions of $GluH^+$ in N_2 at indicated field strength in the reaction chamber.

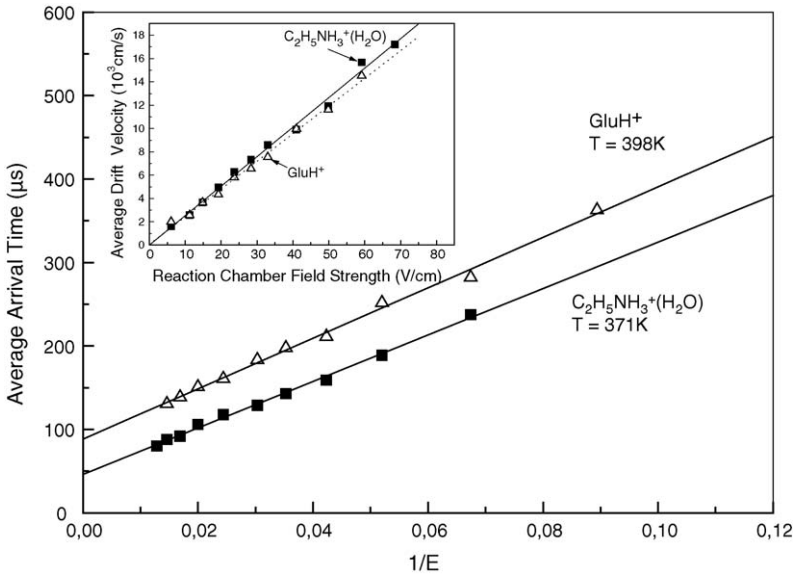

Fig. 3. Variation of average arrival time for $GluH^+$ and $C_2H_5NH_3^+(H_2O)$ in N_2 bath gas with $1/E$ at indicated temperatures and the reaction chamber pressure of 10 mbar. The inset shows the average drift velocities as a function of field strength (see text).

tional to E

$$v_d = \frac{L}{t_d} = KE \quad (1)$$

where the proportionality constant K is the ion mobility [23], t_d the drift time (arrival time) and L is the drift length (RC length = 7 mm). At constant pressure and temperature, the average arrival time t_{av} (center of the ATD peak) should vary as $1/E$. This is indeed demonstrated in the present measurements for $C_2H_5NH_3^+(H_2O)$ and $GluH^+$ (Fig. 3). The intercept of the linear plot of t_{av} versus $1/E$ yields the analyzer time (i.e., the flight time through the instrument and in the detection system). The mean residence time in the RC is obtained by subtracting the analyzer time from the t_{av}. These values in turn yielded the average drift velocities v_{ad} in the N_2 bath gas; the plot of v_{ad} versus E is a linear function as required for low-field drift conditions (see inset of Fig. 3).

The equilibrium studies were performed in the pulsing mode of operation. The equilibrium constants, $K_{n-1,n}$, for each reaction described by the following general equation:

$$BH^+(H_2O)_{n-1} + H_2O \Leftrightarrow BH^+(H_2O)_n \quad (2)$$

were determined from the expression:

$$K_{n-1,n} = \left(\frac{I_n 1000}{I_{n-1} P}\right) \quad (3)$$

where I_n and I_{n-1} are recorded peak areas of the respective ions at equilibrium and P is the partial pressure (mbar) of H_2O in the N_2 bath gas. The ions are hydrated in the RC and reach

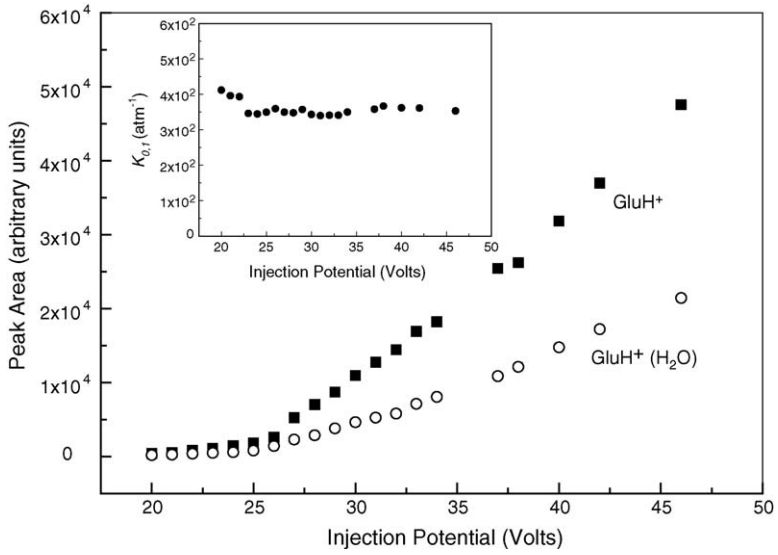

Fig. 4. Variation of peak areas for $GluH^+$ and $GluH^+(H_2O)$ with amplitude of the 60-μs injection pulse applied to the deflection electrode DE at fixed $V_{DE} = V_{IP} = 2014$ V. The inset shows the effect of injection pulse potential on equilibrium constant for the reaction $GluH^+ + H_2O = GluH^+(H_2O)$.

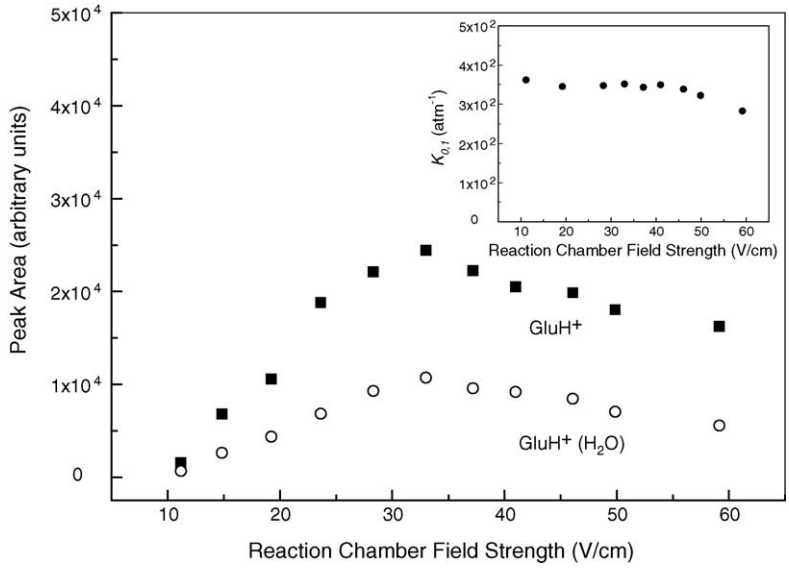

Fig. 5. Variation of peak areas for $GluH^+$ and $GluH^+(H_2O)$ with reaction chamber field strength. The inset shows the effect of field strength on equilibrium constant for the reaction $GluH^+ + H_2O = GluH^+(H_2O)$.

equilibrium prior to being sampled to the mass analysis section of the mass spectrometer. The thermodynamic properties, $\Delta H^\circ_{n-1,n}$ and $\Delta S^\circ_{n-1,n}$, are derived from the temperature dependence of the equilibrium constants using the van't Hoff equation:

$$\ln K_{n-1,n} = \left(\frac{\Delta S^\circ_{n-1,n}}{R}\right) - \left(\frac{\Delta H^\circ_{n-1,n}}{RT}\right) \quad (4)$$

A number of exploratory experiments were performed in order to check the conditions in the FC and RC which may influence the ion intensities and equilibrium constants. The $GluH^+/GluH^+(H_2O)$ system has been chosen to demonstrate the observed effects.

As mentioned earlier, DE acts as an injection potential electrode which drives the ions into RC. In Fig. 4, the peak areas of the ion packets for $GluH^+$ and $GluH^+(H_2O)$ are plotted as a function of amplitude of the injection pulse (60-μs-wide, with periods of 700-μs) applied to the DE when $V_{DE} = V_{IP} = 2014$ V was fixed. These results demonstrate that the ion intensities (integrated peak areas) increase progressively as the pulsing potential increases from ≈25 V, while under these conditions the measured equilibrium constants $K_{0,1}$ remain essentially unperturbed (see inset of Fig. 4). This means that the ion packet gaining excess kinetic energy from the injection potential does not penetrate significantly into the RC before thermalization.

The effect of the reaction chamber field strength on the ion intensities is shown in Fig. 5. The data were obtained at various values of $V_{DE} = V_{IP}$ and by fixing the 60-μs pulsing potential at 38 V. It is seen that the integrated intensities of both $GluH^+$ and $GluH^+(H_2O)$ initially increase but from ≈33 V/cm decrease monotonically with the increasing field strength. However, the equilibrium constants $K_{0,1}$ are found to be essentially independent of $E \leq 40$ V/cm (see inset of Fig. 5). The observed decrease

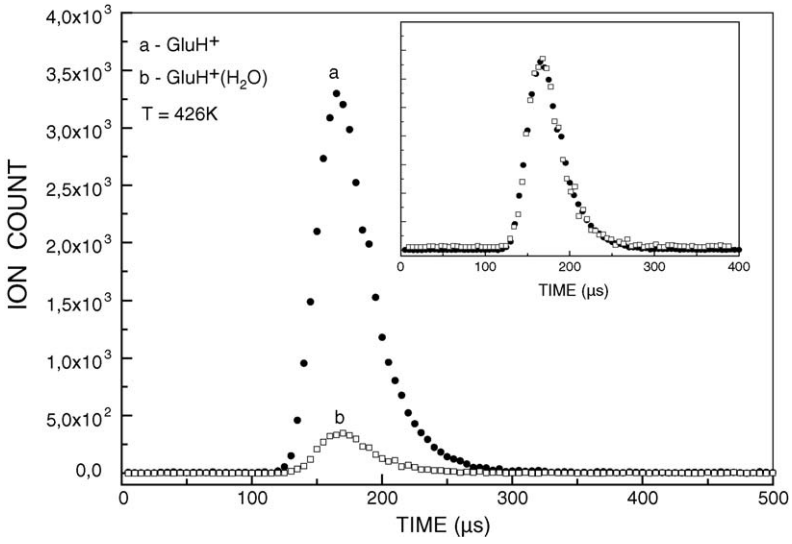

Fig. 6. Arrival time distributions of the reactant, $GluH^+$, and product, $GluH^+(H_2O)$, ions. The inset shows the normalized peak heights.

in intensities with increasing field strength (>33 V/cm) may be due to the time discrimination of ions having a longer residence time during transport into the sampling slit [24].

The equilibrium attainment for the clustering reactions was usually checked by comparing the ATDs of the reactant and product ions. If equilibrium is established, their ATDs must be the same (except for the scaling factor of the peak). This situation is illustrated in Fig. 6 for $GluH^+$ and $GluH^+(H_2O)$. The inset of the figure shows the normalized peak heights for this pair, implying that the $GluH^+/GluH^+(H_2O)$ system is at the hydration equilibrium.

Mass spectra were registered by scanning the spectrometer electromagnet with continuous ion sampling. Typical potentials used with the continuous ion beam were as follows: ESI emitter, approximately 4 kV; PRC and RC, 2 kV; electrode DE, 2050 V; electrode IP, 2016 V. In the pulsing mode of operation, $V_{IP} = V_{DE} = 2014$ V and an injection pulse (+34 V; 60 μs; rise time 10 ns) was applied to the electrode DE with repetition of 1 ms.The pulsing sequence was performed several thousand times to accumulate enough ion counts in time channels for a given mass. The integrated peak area of recorded ion counts is assumed to be proportional to the ion concentrations in the reaction chamber.

Ion detection was provided by a secondary electron scintillation detector of the Daly type [25] with an aluminum conversion dynode using a short rise-time photomultiplier (Hamamatsu R-647-04). The output pulses of the multiplier were counted using a multichannel scaler with dwell time per channel of 1 μs. A total ion count in excess of 10^8 s^{-1} could be achieved.

The RC and FC were pumped via the 7-mm i.d. pumping lead, PL, connected to a capacitance pressure sensor by a 5-mm i.d. tube and to a mechanical forepump (120 L/min) via a tubing having a 12-mm i.d. The pressure in the RC was established by pressure measurements with an MKS capacitance manometer attached near the inlet of the RGI and the outlet of the PL which were found to be 11 and 9 mbar, respectively. The pressure in the RC was assumed to be an average of these two values. The reagent gas mixture consisting of pure N_2 as carrier gas at about 10 mbar and water vapor was supplied to the RC via the reactant gas inlet, RGI, at a flow rate of ∼100 mL/min. Similarly as in the case of Kebarle and co-workers experiments [5], changes in the reagent gas flow rate in the range of 80–160 mL/min were found to have no effect on the observed ion ratios in equilibria determination. Water was introduced into the heated N_2 bath gas flow with a syringe pump. The partial pressure of water vapor was varied over the 0.02–0.25 mbar range. As a general rule, the amount of water injected into the nitrogen gas flow was kept constant throughout the temperature dependence measurements of the equilibrium constants. Water concentrations were controlled continuously with a calibrated temperature and humidity transmitter (Delta OHM, Type DO 9861T, Italy) inserted into the carrier gas flow line. All parts of the gas inlet line were heated.

The reaction chamber temperature can be varied from ambient to 300 °C by means of an electrically heated copper jacket, HJ, surrounding the stainless steel RC block. The temperature was monitored by an iron–constantan thermocouple (with a reference junction in a water–ice bath) which was embedded close to the ion exit slit (see Fig. 1).

2.1. Materials

All fused-silica capillaries were obtained from Polymicro Technologies (USA). Polyimide sealing resin used for the ESI emitter was obtained from Shinetsu (Japan); graphite powder, 1–2 μm particle size, was obtained from Aldrich. Alkylamines and amino acids (obtained from Aldrich) and the dipeptides γ-Glu-Met (obtained from Bachem, Philadelphia, USA) and Met-Glu (obtained from Serva, Germany) were used as received. Water was deionized with a Millipore Purifier, Type Elix 5 (Austria).

3. Results and discussion

In order to examine the reliability of our results obtained with our ESI pulsed ion source, the thermochemical data of a few protonated alkylamines have been determined. These systems were chosen because they have been well characterized by several investigators [9–12] and the results are of interest in connection with the hydration of the protonated amino acids and peptides. A comparison of the present results with previous measurements using the high-pressure mass spectrometric techniques with pulsed-electron [10,11] and ESI [9] ionization methods is shown in Table 1. The van't Hoff plot for the hydration of $C_2H_5NH_3^+$ shown in Fig. 7 is an illustration of the results on which the data in Table 1 were acquired. As can be seen, there is a reasonably good agreement between the present results and earlier data. In the case of $C_2H_5NH_3^+$, there are significant differences in the corresponding $\Delta S^\circ_{n-1,n}$ values obtained in the different experiments, but it is hard to rationalize these discrepancies. Unfortunately, measurements of equilibria were possible only for $n < 2$, because determination of the hydration enthalpies for higher steps requires subambient reaction temperatures. These are as yet not accessible with the present reaction chamber. Therefore, only the thermochemical data given in Tables 1 and 2 could be obtained.

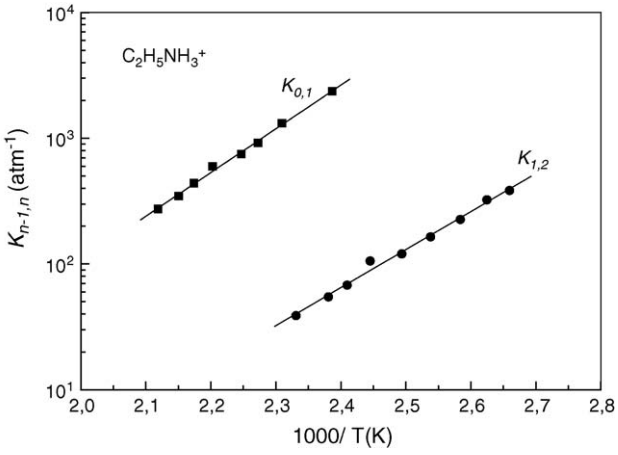

Fig. 7. van't Hoff plots of equilibrium constants for the (0,1) and (1,2) hydration of $C_2H_5NH_3^+$.

Table 1
Thermochemical data[a] for hydration of protonated alkylamines in gas-phase reactions $M^+(H_2O)_{n-1} + H_2O = M^+(H_2O)_n$

M	$n-1,n$	$-\Delta H^\circ_{n-1,n}$ (kcal/mol)	$-\Delta S^\circ_{n-1,n}$ (cal/(mol K))[b]	$-\Delta G^\circ_{n-1,n}$ (kcal/mol)[c]	Ref.
$(CH_3)_2NH_2^+$	0,1	15.0 ± 0.8	22.4 ± 2.0	8.3 ± 1.4	
		14.4 ± 0.4	22.1 ± 1.3	7.8 ± 1.3	[9]
		15.0 ± 0.5	22.9 ± 1.0	8.2 ± 0.7	[11]
				9.1	[12]
	1,2	13.3 ± 1.0	26.3 ± 2.5	5.5 ± 1.7	
		13.8 ± 0.7	26.8 ± 2.3	5.8 ± 1.4	[9]
		13.5 ± 0.5	24.7 ± 1.0	6.1 ± 0.7	[11]
				6.2	[12]
$C_2H_5NH_3^+$	0,1	16.0 ± 0.4	22.6 ± 0.9	9.3 ± 0.7	
		14.2 ± 0.2	19.5 ± 0.4	8.3 ± 0.3	[9]
		17.5 ± 0.5	25.9 ± 1.0	9.8 ± 0.7	[11]
		17.5 ± 0.5	25.9 ± 0.9	9.8 ± 0.5	[10]
	1,2	13.9 ± 0.5	25.0 ± 1.2	6.5 ± 0.9	
		12.7 ± 0.2	21.6 ± 0.8	6.3 ± 0.5	[9]
		14.7 ± 0.5	29.7 ± 1.0	5.8 ± 0.7	[11]
		14.7 ± 0.2	29.7 ± 0.7	5.8 ± 0.3	[10]
n-$C_4H_9NH_3^+$	0,1	15.0 ± 1.0	24.2 ± 3.0	7.8 ± 2.1	
		16.0 ± 0.5	26.4 ± 1.5	8.1 ± 0.9	[9]
	1,2	12.2 ± 1.0	24.0 ± 2.0	5.1 ± 1.6	
		13.6 ± 0.3	26.0 ± 1.1	5.8 ± 0.7	[9]

[a] Standard pressure is 1000 mbar.
[b] Results given to the temperature of the van't Hoff plot. However, since the ΔS° dependence upon the temperature is small, ΔS° values are approximately equal to those at 298 K.
[c] ΔG° at 298 K.

The van't Hoff plots of equilibrium constants for the protonated amino acids and dipeptides are shown in Fig. 8. A weighted least-squares fit of the plots yields the thermochemical quantities for these systems listed in Table 2. Generally, the hydration enthalpies of the protonated amino acids and dipeptides obtained in the present work are similar to those found for a large number of protonated alkylamines whose values are in the range of 14–16 kcal/mol for the first, and 12–15 for the second water molecule (Table 1) [6,9–11,17]. There is an obvious disagreement between the $\Delta H^\circ_{0,1}$ and $\Delta S^\circ_{0,1}$ values obtained in the present work and earlier data reported for $ValH^+$, but good agreement in $\Delta G^\circ_{0,1}$ (Table 2) [14]. The $\Delta H^\circ_{0,1}$ values for dipeptides $(Glu\text{-}Met)H^+$ (14.2 kcal/mol) and $(Met\text{-}Glu)H^+$ (13.8 kcal/mol) are close to that measured by Bowers and co-workers [17] for $(Ala\text{-}Ala)H^+$ (14.8 kcal/mol), although there are some differences in $\Delta S^\circ_{0,1}$ (see Table 2).

The attachment energy of the first H_2O molecule to $GluH^+$ is smaller than to $MetH^+$ and $ValH^+$ (Table 2). In all these systems, the most favorable protonation site is the $-NH_2$ group [26]. The observed difference in the water binding energies can be rationalized in terms of differences in the gas-phase basicity (GB) or proton affinity (PA) of these systems. Theoretical [26] and exper-

Table 2
Thermochemical data[a] for gas-phase hydration of protonated amino acids and dipeptides

Ion	$n-1,n$	$-\Delta H^\circ_{n-1,n}$ (kcal/mol)	$-\Delta S^\circ_{n-1,n}$ (cal/(mol K))[b]	$-\Delta G^\circ_{n-1,n}$ (kcal/mol)[c]	Ref.
$GluH^+$	0,1	13.1 ± 0.4	22.6 ± 1.0	6.4 ± 0.7	
	1,2	12.8 ± 0.7	25.6 ± 2.0	5.2 ± 1.3	
$MetH^+$	0,1	15.8 ± 0.5	28.7 ± 1.2	7.2 ± 0.9	
	1,2	14.7 ± 0.7	31.4 ± 2.0	5.3 ± 1.3	
$ValH^+$	0,1	15.1 ± 0.5	24.6 ± 1.0	7.8 ± 0.8	
	0,1	19.3 ± 1.0	36.3 ± 3.0	8.4 ± 2.0[d]	[14]
	1,2	13.8 ± 0.5	27.6 ± 1.4	5.6 ± 0.9	
$(Glu\text{-}Met)H^+$	0,1	14.2 ± 0.8	34.0 ± 1.2	4.1 ± 0.8	
$(Met\text{-}Glu)H^+$	0,1	13.8 ± 0.8	31.4 ± 2.0	4.4 ± 1.4	
$(Ala\text{-}Ala)H^+$	0,1	14.8 ± 0.3	24.7 ± 1	7.4 ± 0.1	[17]

[a] Standard pressure is 1000 mbar.
[b] Results given to the temperature of the van't Hoff plot. However, since the ΔS° dependence upon the temperature is small, ΔS° values are approximately equal to those at 298 K.
[c] ΔG° at 298 K.
[d] ΔG° at 300 K.

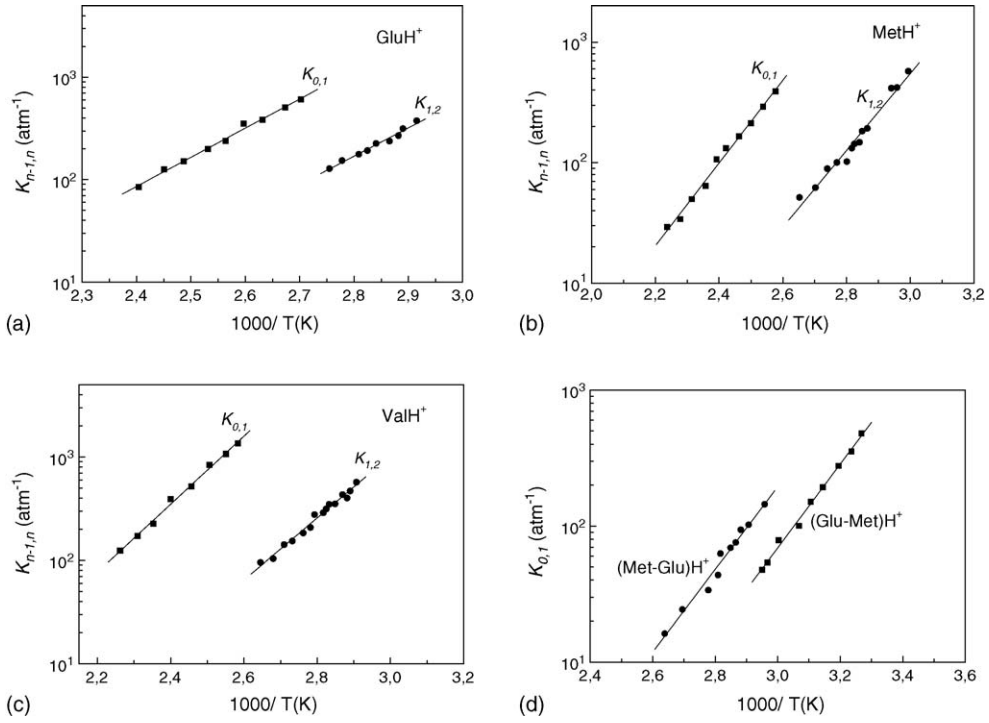

Fig. 8. van't Hoff plots of equilibrium constants for the gas-phase reactions $B^+(H_2O)_{n-1} + H_2O = B^+(H_2O)_n$, where B equals (a) $GluH^+$; (b) $MetH^+$; (c) $ValH^+$; (d) $(Glu\text{-}Met)H^+$ and $(Met\text{-}Glu)H^+$.

imental [27,28] studies show that PA(Glu) > PA(Met) > PA(Val). Therefore, the residual charge density on the protic hydrogens in the $-NH_3^+$ group is expected to be smaller and the hydrogen bonding to H_2O should be weakened with increasing PA's of these compounds.

Fig. 9 shows the plot of free energy changes $-\Delta G^\circ_{0,1}(BH^+)$ for the addition of the first water molecule to amino acids versus the GB values. Since there are significant differences between the GBs (or PAs) experimentally measured by different techniques and originating from different laboratories [27–29], for the gas-phase basicities we take the "best" GB values derived by Harrison [29]. An approximately linear correlation exists between the GBs and $-\Delta G^\circ_{0,1}(BH^+)$ obtained in this work for $GluH^+$, $MetH^+$ and $ValH^+$, and reported in the literature for several amino acids [5,14,15]. In contrast to alkylamines, different protonation sites and side chains are present in the amino acids shown in Fig. 9. Theoretical calculations [26] at the MP2(fc)/6-311 + G**//HF/6-31G* + ZPVE(HF/6-31G* level of theory predict the protonation site at the N-terminus for Gly, Val, Glu, Met, and at the side chain in Lys, and the quanidinium group in Arg. The observed correlation (Fig. 9) clearly indicates that the side chains delocalize the positive charge density on the protonated groups and have a dominating effect on the hydration energies of amino acids. Functional groups present in side chains of amino acids and peptides can be involved in both the intramolecular hydrogen bonds and intermolecular hydrogen bonding interactions with the H_2O solvent molecule [13,19]. In effect, a part of the positive charge on the protonated group is transferred to a side chain, resulting in a decrease of the electrostatic interaction between the charged group and the H_2O solvent molecule.

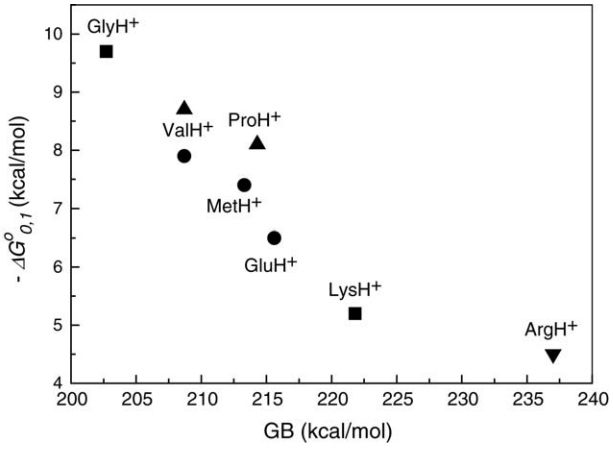

Fig. 9. Correlation between free energy, $-\Delta G^\circ_{0,1}$, at 293 K and gas-phase basicity, GB(B), for the hydration of protonated amino acids: $BH^+ + H_2O = BH^+(H_2O)$. The protonated basis, BH^+, are indicated in the figure. The GB(B) values are taken from ref. [29]. Hydration free energies for $GluH^+$, $MetH^+$ and $ValH^+$, present work (●); $GlyH^+$ and $LysH^+$, ref. [5] (■); $ProH^+$ and $ValH^+$, ref. [14], (▲); $ArgH^+$, obtained from $\Delta H^\circ_{0,1}$ and $\Delta S^\circ_{0,1}$ values reported in ref. [15] (▼).

The hydration enthalpies, $\Delta H^\circ_{0,1}$ and $\Delta H^\circ_{1,2}$, given in Table 2 show that the interactions of the second water molecule with the protonated amino acids are somewhat weaker than those of the first, although the values are slightly obscured if one takes the experimental errors into consideration. It is very likely that both water molecules bind directly to the protonated group. The molecular mechanics calculations performed by Bowers and coworkers [17] for singly and doubly protonated bradykinin predict that one or two water molecules have a preference for adding

to a charged site. Slightly lower values of $\Delta H^{\circ}_{1,2}$ compared to those of $\Delta H^{\circ}_{0,1}$ (Table 2) can be attributed to the decrease in the amount of charge present on the protonated group with the addition of the second water molecule. Such an effect has been quantitatively reproduced for $CH_3NH_3^+(H_2O)_n$, $n = 1$–4, by Liu et al. [13], based on natural bond analysis (NBO).

Theoretical calculations, performed by Sun et al. [30] at the B3LYP/6-31 + G** level of theory, predict that GluH$^+$ exhibit a cyclic structure due to the formation of intramolecular hydrogen bonds; the lowest energy structure is characterized by one very short (and strong) hydrogen bond between the protonated amine group and the carbonyl oxygens, $N^+-H\cdots O{=}C$ (see structure **I**). The first and the second water molecules could be inserted between the hydrogen bonds, $N^+-H\cdots OH_2\cdots O{=}C$, to form a structure such as **II**. However, theoretical calculations are needed to verify this structure.

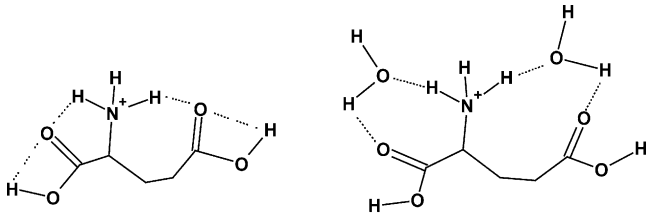

I II

For MetH$^+$ and ValH$^+$, the $\Delta H^{\circ}_{n-1,n}$ values are very close to those for the protonated alkylamines $C_mH_{2m+1}NH_3^+$, which for $m = 3$–10 are in the range of 14.8–16 kcal/mol for the first, and 11.6–13.9 kcal/mol for the second water molecule (see Tables 1 and 2) [6,9,13,17]. Moreover, the $\Delta G^{\circ}_{0,1}$ and $\Delta G^{\circ}_{1,2}$ values for the systems are similar, all falling between the limits 7.2–8.8 kcal/mol for the (0,1) and 5.3–6.7 kcal/mol for the (1,2) hydration. This observation suggests that in the case of the amino acids with the non-polar side chains, such as MetH$^+$ and ValH$^+$, the amount of charge remaining at the $-NH_3^+$ group is comparable to that in alkylamines with C_3–C_{10}.

The $\Delta H^{\circ}_{0,1}$ values for the hydration of (Glu-Met)H$^+$ and (Met-Glu)H$^+$ are almost equal, and close to that for GluH$^+$, but the $\Delta S^{\circ}_{0,1}$ values in the case of dipeptides are "more negative" (Table 2). The higher (~35%) average $\Delta S^{\circ}_{0,1}/\Delta H^{\circ}_{0,1}$ ratio found for dipeptides than for amino acids indicates that water molecule in the (Glu-Met)H$^+$ and (Met-Glu)H$^+$ systems is bound more tightly than in the singly hydrated amino acids. This situation can be explained by the fact that (Glu-Met)H$^+$ and (Met-Glu)H$^+$ have the longer chains compared to amino acids and therefore a greater flexibility to form long range hydrogen bonding. The carbonyl >C=O groups present in these systems can be engaged in the intramolecular (and possibly intermolecular) hydrogen bonding with the protonated amino group leading to the loss of freedom of motions of the H_2O molecule.

The hydration energies $-\Delta G^{\circ}_{0,1}$ for (Glu-Met)H$^+$ (4.2 kcal/mol) and (Met-Glu)H$^+$ (4.6 kcal/mol) at 293 K are close to that for (Gly-Lys)H$^+$ (4.9 kcal/mol) reported by Kebarle and co-workers [5], but significantly lower than those obtained for the smaller dipeptides, (Gly-Gly)H$^+$ (8.8 kcal/mol) [5] and (Ala-Ala)H$^+$ (7.6 kcal/mol) [17]. Fig. 10 shows the relation between $-\Delta G^{\circ}_{0,1}$ values and a number of carbon atoms

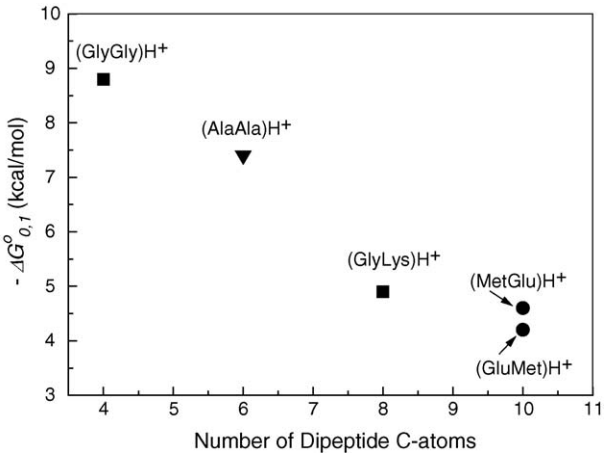

Fig. 10. Plot of free energy, $-\Delta G^{\circ}_{0,1}$, at 293 K for the hydration of protonated dipeptides versus a number of dipeptide C-atoms. The $-\Delta G^{\circ}_{0,1}$ values for (Glu-Met)H$^+$ and (Met-Glu)H$^+$, present work (●); (Gly-Gly)H$^+$ and (Gly-Lys)H$^+$, ref.[5] (■); (Ala-Ala)H$^+$, ref.[17] (▼).

available in dipeptides. It is seen that the hydration energy decreases as the number of C-atoms increases. This effect can be explained by increasing intramolecular charge delocalization in the systems, and as a consequence of this a decrease of the net charge density on the ionized group, with increasing system size.

4. Conclusions

An ion source has been constructed which allows to produce a continuous ion beam by electrospray ionization at atmospheric pressure, transfer it through a pressure reducing interface and inject it into the reaction chamber in a pulsed mode where the gas-phase ion–molecule equilibria can be determined at 10 mbar. A number of operating parameters have been evaluated. The usefulness of this source for the quantitative measurements of the gas-phase thermodynamic properties of solvation, especially the hydration of biomolecules such as amino acids and small peptides has been demonstrated.

Acknowledgment

This study was supported by Grant No. 3T09A02728 from the Ministry of Scientific Research and Information Technology (Poland).

References

[1] J.B. Fenn, M. Mann, C.K. Meng, S.F. Wong, C.M. Whitehouse, Science 88 (1984) 4451.
[2] S.W. Lee, P. Freivogel, T. Schindler, J.L. Beauchamp, J. Am. Chem. Soc. 120 (1998) 11758.
[3] S.E. Rodriguez-Cruz, J.S. Klassen, E.R. Williams, J. Am. Soc. Mass Spectrom. 10 (1999) 958.
[4] D. Zhan, J.B. Fenn, Int. J. Mass Spectrom. 219 (2002) 1.
[5] J.S. Klassen, A.T. Blades, P. Kebarle, J. Phys. Chem. 99 (1995) 15509.
[6] A.T. Blades, J.S. Klassen, P. Kebarle, J. Am. Chem. Soc. 118 (1996) 12437.
[7] J. Woenckhaus, Y. Mao, M.F. Jarrold, J. Phys. Chem. B 101 (1997) 847.

[8] T. Wyttenbach, P.R. Kemper, M.T. Bowers, Int. J. Mass Spectrom. 212 (2001) 13.
[9] J.J. Gilligan, F.W. Lampe, V.Q. Nguyen, N.E. Vieira, A.L. Yergey, J. Phys. Chem. A 107 (2003) 3687.
[10] Y.K. Lau, P. Kebarle, Can. J. Chem. 59 (1981) 151.
[11] M. Meot-Ner (Mautner), J. Am. Chem. Soc. 106 (1984) 1265.
[12] C.M. Banic, J.V. Iribarne, J. Chem. Phys. 83 (1985) 6432.
[13] D. Liu, T. Wyttenbach, M.T. Bowers, Int. J. Mass Spectrom. 236 (2004) 81.
[14] M. Meot-Ner, F.H. Field, J. Am. Chem. Soc. 96 (1974) 3168.
[15] T. Wyttenbach, M.T. Bowers, Top. Curr. Chem. 225 (2003) 207.
[16] M. Kohtani, M.F. Jarrold, J. Am. Chem. Soc. 124 (2002) 11148.
[17] D. Liu, T. Wyttenbach, P.E. Barran, M.T. Bowers, J. Am. Chem. Soc. 125 (2003) 8458.
[18] T. Wyttenbach, B. Paizs, P. Barran, L. Breci, D. Liu, S. Suhai, V. Wysocki, M.T. Bowers, J. Am. Chem. Soc. 125 (2003) 13768.
[19] T. Wyttenbach, D. Liu, M.T. Bowers, Int. J. Mass Spectrom. 240 (2005) 221.
[20] J. Woenckhaus, R.R. Hudgins, M.F. Jarrold, J. Am. Chem. Soc. 119 (1997) 9586.
[21] H. Wincel, Int. J. Mass Spectrom. Ion Processes 175 (1998) 283.
[22] S. Nilsson, M. Wetterhall, J. Bergquist, L. Nyholm, K.E. Markides, Rapid Commun. Mass Spectrom. 15 (2001) 1997.
[23] E.W. McDaniel, Drift Tube Studies of the Transport Properties and Reactions of Slow Ions in Gases, North-Holland Publ. Company, Amsterdam–London, 1969 (Chapter 1).
[24] G. Sroka, C. Chang, G.G. Meisels, J. Am. Chem. Soc. 94 (1972) 1052.
[25] N.R. Daly, Rev. Sci. Instrum. 31 (1960) 264.
[26] Z.B. Maksić, B. Kovačević, Chem. Phys. Lett. 307 (1999) 497.
[27] G. Bojesen, T. Breindahl, J. Chem. Soc. Perkin 2 (1994) 1029.
[28] G.S. Gorman, J.P. Speir, C.A. Turner, I.J. Amster, J. Am. Chem. Soc. 114 (1992) 3986.
[29] A.G. Harrison, Mass Spectrom. Rev. 16 (1997) 201.
[30] W. Sun, G.R. Kinsel, D.S. Marynick, J. Phys. Chem. A 103 (1999) 4113.